VILNIUS TECH
Vilnius Gediminas Technical University

Journal of Environmental Engineering and Landscape Management
ISSN 1648–6897 / eISSN 1822-4199
2023 Volume 31 Issue 3: 186–195
https://doi.org/10.3846/jeelm.2023.19468

SHORT-TERM COASTAL LANDSCAPE EVOLUTION IN CIREBON BAY USING COASTLINE ENVIRONMENT ANALYSIS

Raden Yudi PRATAMA[1, 2*], Nana SULAKSANA[1], Emi SUKIYAH[1], Teuku Yan Waliana Muda ISKANDARSYAH[1], Franto NOVICO[3, 4], Zulfahmi ZULFAHMI[5], Evi Hadrijati SUDJONO[3, 4], Duddy RANAWIJAYA[4]

[1]*Faculty of Geological Engineering, Universitas Padjadjaran, Jl. Raya Bandung Sumedang KM 21, 45363 Jatinangor, Indonesia*
[2]*Human Resources Development Center for Geology Mineral and Coal, Ministry of Energy and Mineral Resources, 40211 Bandung, Indonesia*
[3]*Research Center for Geological Disaster, National Research and Innovation Agency, 40135 Bandung, Indonesia*
[4]*Marine Geological Institute, Ministry of Energy and Mineral Resources, 40174 Bandung, Indonesia*
[5]*Research Center for Geological Resources, National Research and Innovation Agency, 40135 Bandung, Indonesia*

Received 25 September 2022; accepted 30 May 2023

Highlights

- The article uses geoscience data as an integrated approach to providing new insight into coastal landscape analysis.
- The vertical sediment composition shows the influence of the marine regime plays an important role in the process of longshore sediment transport (LST).
- Geospatial analysis proves a strong correlation to sedimentation rate based on ^{210}Pb.

Abstract. The landscape of Java's north coast is dominated by a mild slope covered by soft sediment, which faces many environmental issues. These issues have been identified, and the simple technique of overlaying Landsat imagery shows the evolution of the landscape along the coast. Survey campaigns in 2006 and 2018 verified the Landsat overlay, and the ^{210}Pb dating analysis aids in describing the sedimentation rate along the coast. The results demonstrate that accretion evolution dominates exclusively in Cirebon's coastline landscape, with coastal gains reaching 1463.88 ha over four decades and the sediment rate from 1977–1997 estimated at 0.27–0.33 cm/year. Compared to the earlier decade, the recent two periods from 1998 to 2018 demonstrate a more extensive desire for progressive accretion affected by the longshore sediment transport. Hence, special attention should be paid to the northern coast of Java to estimate the sedimentation rate and the advanced coast.

Keywords: landscape evolution, north Java coast, Cirebon Bay, geoscience data, integrated data, advance coast.

Introduction

The north coast of Java is Indonesia's most populated and developed area (Jones, 2013; Novico et al., 2021c). However it is still vulnerable to disaster, including Cirebon bay as it is located on the north coast of Java (Figure 1). The various issues along the coastal area have been studied in other parts of the world (Dadson et al., 2016; Dolan et al., 1991; Gardel & Gratiot, 2006; Kumar et al., 2010; Kurt et al., 2010; Li & Gong, 2016; Rizzo & Anfuso, 2020; Vos et al., 2019; Williams, 2013; Xu, 2018), as is the case in Indonesia such as back and forth coastal area, inundation and subsidence (Novico et al., 2021c; Andreas et al., 2018). The essential oceanic processes influencing the morphological development of coastlines are wind waves and wave-driven nearshore currents (Dean & Dalrymple, 2001). Much energy from waves and currents is transferred directly to the seabed in shallow water. This process causes sediment transport and changes in the seabed through different bed forms at different spatial and temporal scales (Kaczmarek et al., 2005). The longshore current, caused by waves breaking at an angle to the coast,

*Corresponding author. E-mail: *yudi.prat@gmail.com*

moves the longshore sediment transport (LST) (Longuet-Higgins, 1970; van Rijn et al., 2003). Unbalance LST will create the coastal retreat and advance, creating a problem for coastal communities (Pilkey & Cooper, 2014). Besides, issues regarding coastal morphology have been studied by (Kumar et al., 2010; Pilkey & Cooper, 2014; Toorman et al., 2018, related to storm by (Höffken et al., 2020), and land use development (Dean & Dalrymple, 2001; Quang et al., 2021; Thieler et al., 2009). Those issues related to anthropogenic heritage also occurred in Cirebon (Novico, 2006). However, in the long-term geological scale, the dominance of tectonic and eustatic level also play a role in coastal evolution, as mentioned by a previous study (Menier et al., 2010; Meyssignac & Cazenave, 2012; Pian & Menier, 2011; Sathiamurthy & Voris, 2006; Williams, 2013).

Undoubtedly, a dynamic coastline study is needed to understand coastal evolution comprehensively. However, due to a different point of view, shoreline dynamics are only explored by a few variables in the typical investigation. Hence, our main objective is to reveal the phenomenon of short-term coastal dynamics in Cirebon bay by organising some proxies to explore the coastal evolution in Cirebon waters. The four decades of satellite images are used as benchmarks of coastline calculation in this research. Due to the lack of a time series data set of field measurements, the short-term marine acquisition of bathymetry data, sub-bottom profile, and lithology, aided by radioactive analysis ^{210}Pb, were used to verify the coastal evolution.

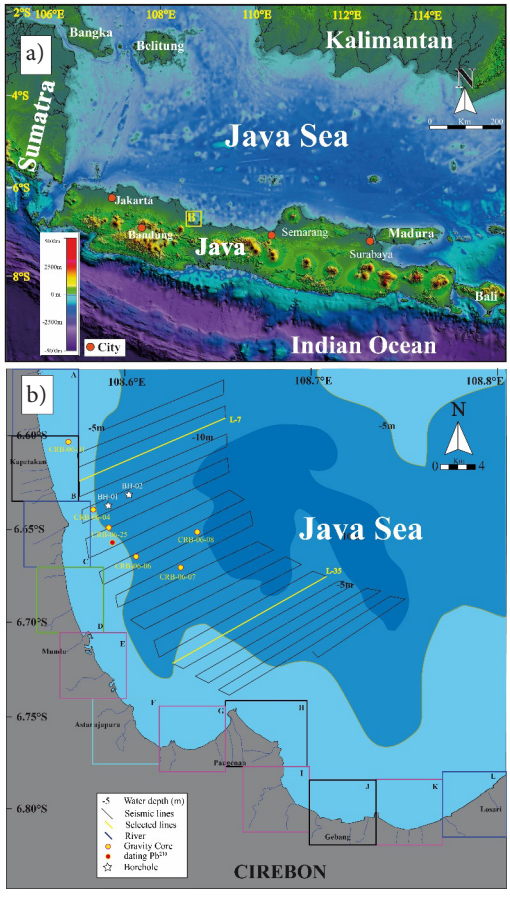

Figure 1. a) Study locations on a map Cirebon Regency are situated in Java's northern coastline zone; b) Cirebon is a reasonably flat flood plain of the Cimanuk-Cisanggarung deltaic system (grey color), with bathymetry of Cirebon waters (blue colour), selected seismic lines (yellow lines), core drilling (white star), and sampling sediments (yellow node)

1. Regional setting and sediment distribution

The physiographic arrangement of Cirebon Bay, from the southern sections to the northern areas, encompasses the complexity of the Southern Java compression zone, the West Java volcanic region, and the extension back-arc of the Java Sea. The extensional faulting dominates the coastline of North-West Java, with minimal compressional structure (Darman & Sidi, 2000; Sathiamurthy & Voris, 2006). It has been formed since the early Tertiary by continuous subsidence and southward tilting of the Sunda plate (Hamilton, 1979). The morphology of the coastal area in Cirebon bay has irregularity of the coastline where the west part tends to the north, then the east. Theoretically, the western part will get less current flux from offshore than the east when the west monsoon. Besides, the mild slope of the coastal zone preserves the homogeneous alluvial deposit along the coast, which is less than 17% (Novico, 2006).

Cirebon's coastal area is covered by unconsolidated sediment (Silitonga & Masria, 1978) and soft sediment (Salahuddin et al., 2001). The lithology of the onshore area around Cirebon is divided into four units: alluvial (Qa), Mt. Ceremai eruption (Qvr), Gintung Formation (Qpg), and Kalibiuk Formation (Tpb), as shown in Figure 2. Onshore lithology shows the dominance of volcanic products. The coastline is covered by alluvial material of soft and loose sediment material typical of marine deposits. In addition, Cirebon Bay consists of two lithologies, mud (Z) and slightly gravelly sandy mud, that might accumulate mixed transport onshore and offshore.

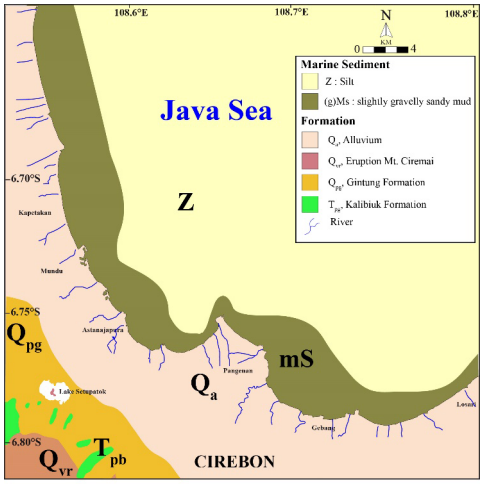

Figure 2. Modification map of seafloor sediment distribution (Salahuddin et al., 2001) and onshore lithology in the Cirebon Area (Silitonga & Masria, 1978). The Q_a is identified as alluvium containing that cohesive and loose sediment

2. Materials and methods

Integrated data consisting of time-series Landsat imagery, bathymetry survey which used a single beam Odom Hydrotrac I, 200 kHz echo sounders, sediment cores by rotary drilling, sediment sampling by gravity core, ^{210}Pb dating, high-resolution single-channel seismic analogue records (HRSS) by applied the uniboom boomer system, and hydrodynamic model data aided by Mike 21HDFM. The survey campaign was conducted in 2006, and bathymetry was updated in 2018. The Landsat imageries obtained from the United States Geological Survey cover the years 1978–1988, 1988–1998, 1998–2008, and 2008–2018 (Table 1). Pre-processing procedures are completed by correcting the radiometric and atmospheric. It was analysed using ENVI software for radiometric and FLAASH model for atmospheric. It is a standard procedure to extract the shoreline data from Satellite images time series and the shoreline position derived from visual and by applying digital image-processing techniques (Kumar et al., 2010; Xu, 2018). Data from Landsat images were georeferenced and reformatted to a GIS environment. Satellite imagery is acquired at any stage of the tide, so tidal corrections are needed (Boak & Turner, 2005; Kumaravel et al., 2013). The process from georeferencing to visual and digital image interpretation and conversion raster to vector and GIS analysis is done to get shoreline data (Kumar et al., 2010). We use ENVI software and ArcGIS to extract digitally and process for LANDSAT time series analysis. We applied some bands, which are Landsat 2 (1978) by applying band RGB 654, Landsat 5 (1988) 457, Landsat 5 (1998) 457, Landsat 5 (2008) 457, and Landsat 8 (2018) 653. According to the objective of this study, to identify coastal landscape evolution, an overlying all Landsat series was logically engaged, followed by mapping the coastline zonation of accretion and abrasion.

Therefore, the Digital Shoreline Analysis System (DSAS) tool in ArcGIS has been applied to assist the time series evolution of the coastline changing along the Cirebon coast. This tool is commonly used to analyse accretion abrasion (Quang et al., 2021). Within this analysis, some parameters can be explored, such as End Point Rate (EPR), Linear Regression Rate (LRR), Shoreline Change Envelope (SCE), and Net Shoreline Movement (NSM). Because it depends on the oldest and youngest shorelines (Thieler et al., 2009), the EPR parameter often indicates an overall change over time. EPR can be used to examine two shorelines. However, for more than two shorelines, LRR is more precise and objective. Positive accretion numbers and negative abrasion values can be found in the EPR and LRR results (Quang et al., 2021).

Moreover, in the sediment deposition or erosion framework, the evidence of coastal dynamic could logically be pertained to some vertical variations of depositional environments by interpreting seismic facies and sediment grain size distribution (Catuneanu et al., 2009; Martínez-Carreño & García-Gil, 2017; Menier et al., 2010; Novico et al., 2021a, 2021b). As a result, a 225 km long high-resolution seismic reflection campaign survey was completed in 27 lines using a unit pulse boomer EG&G-234 and a Benthos ten element hydrophone. Two seismic lines, L-7 and L-35, were selected (Figure 1b) to identify the sediment succession of representative uppermost sequences and the thickness of the depositional trend. Furthermore, six selected short gravity cores and two drillings' cores were analysed for the lateral-vertical distribution of lithology and grain sizes (Figure 1b). Lateral lithology distribution is needed to achieve the modern lithology variation along the Cirebon coastline and is used to verify lithological texture conformity between coastal and offshore lithology. Its variations graphs are a proxy to observe the accords with coastal dynamic. In addition, selected samples were examined using ^{210}Pb dating analysis spectrometer gamma (92x spectrum meter, ortec) in the Center for Science and Acceleration Technology, National Nuclear Power Agency (PSTA BATAN) laboratory Yogyakarta Indonesia was completed using a sediment core to calculate the rate of sedimentation. All data from those proxies is processed using the flow chart in Figure 3 until the final results are obtained, which are depicted in map abrasion-accretion and calculation graphs.

3. Results

3.1. DSAS analysis of interdecadal coastal evolution

According to DSAS analysis (Figure 4), the blue area of the advance zone dominated from 1978 to 1988 and again from 2008 to 2018. However, between 1988 and 2008, the red area indicated a slight erosion along the coast of Cirebon Bay.

Based on the DSAS analysis (Table 2), it can be determined that the first decade of 1978 to 1988 presented coastal accretion with an average rate of 11.08 m yr^{-1} (EPR), and NSM revealed an average shoreline change of 110.49 m. In the following decades, from 1988 to 2008, the

Table 1. Landsat data for Cirebon Area

Images	Sensor	Data	Path Row	Local Time	Resolution	Tidal Height
Landsat 2	MSS.	09/25/1978	129065	08h52′08″	80 m	0.083
Landsat 5	TM	09/14/1988	121065	09h32′03″	30 m	0.012
Landsat 5	TM	08/09/1998	121065	09h32′42″	30 m	–0.012
Landsat 5	TM	09/21/2008	121065	09h39′11″	30 m	0.154
Landsat 8	OLI_TIRS	10/03/2018	12165	09h54′03″	30 m	0.196

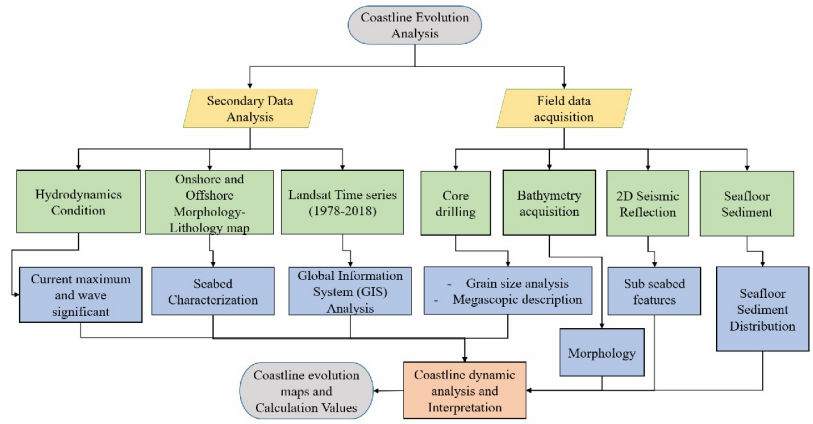

Figure 3. The investigation began with a rounded grey rectangle representing an evolution analysis of a coastline. It comprises two major data mentioned in the yellow parallelogram as input. Each data need the acquisition process mentioned in the green rectangle, and the subject process for each parameter indicated in the blue rectangle. The following process is displayed in an orange rectangle where all those parameters are linked to yield the dynamic of the coastline, which is described by calculation values and coastline evolution maps in a grey rounded rectangle

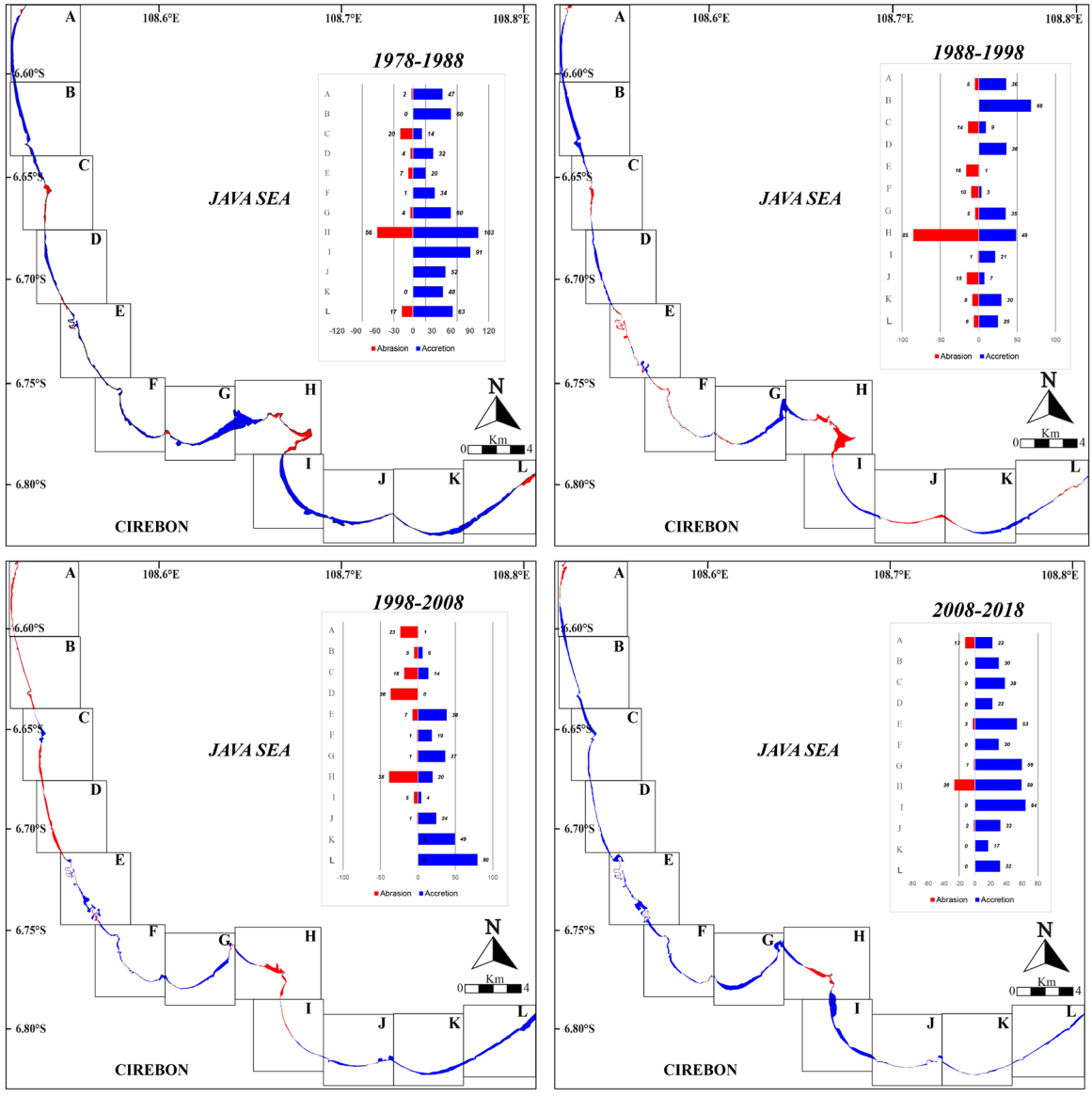

Figure 4. Total abrasion and accretion area among each zone during four decades

Table 2. The coastal dynamic during 1978–2018

No	Period	Average EPR (m yr^{-1})	Average NSM (m)	Advance deposition (ha)	Retreat erosion (ha)
1	1978–1988	11.08	110.49	623.51	111.87
2	1988–1998	4.73	46.81	320.12	164.89
3	1998–2008	2.71	27.43	291.98	136.43
4	2008–2018	5.02	50.31	458.62	44.48

magnitude of sedimentation decreased, and the average EPR was 4.73–2.71 m yr^{-1} and NSM 46.81–27.43 m. This means that it reduced to 30–50% from the first decade. Furthermore, the last decade, 2008–2018, shows that average EPR and NSM rebounded to 5.02 m yr^{-1}, 50.31 m.

3.2. Interpretation of seismic unit

The deposition and erosion pattern around the coastline naturally relates to the sediment transport around the coast. Although accretion-erosion dominates in a short-term period of four decades, at least it can be seen as a trend of sediment accumulation from the sub-bottom profile data around the Cirebon waters. Figure 5a–b illustrates four sedimentary units obtained from line-7 and line-35 seismic data. To reveal the phenomenon of the sedimentation process, seismic profiles were analysed in terms of continuity, amplitude, configuration, and termination of reflectors (Catuneanu et al., 2009; Vail et al., 1977). All units are featured by dominated parallel laminations and acoustic turbidity that mask some of the reflector's records (Menier et al., 2010; Novico et al., 2022b).

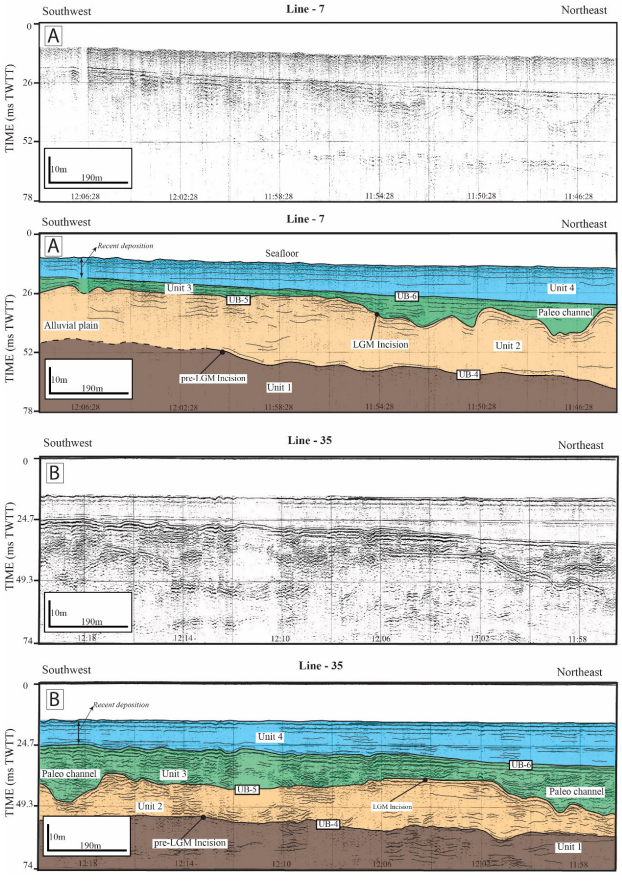

Figure 5. The seismic data and its interpretation (a) line L-7 shows unit 4 has a deposition trend, paleochannel in unit 3, and LGM boundary is UB-2. It is located in the northern part of the bay (b) line L-35 and shows the same pattern in the southern part of the bay

Unit 1 (U1) corresponds to the oldest sediment deposit body reached by this seismic data acquisition, Figure 8. This unit is located ±50 ms TWT from surface water. The thickness of Unit 2 (U2) varies greatly, ranging from about 10 ms TWT to 30 ms TWT. Unit 3 (U3), which has a thickness ranging from 2 ms TWT to 23 ms TWT and is laid on a very irregular channelling erosional surface, has a flat upper layer that covers a prograding system in some areas of the unit's distribution (Figure 5). The base of U3 is a large incision that intersects the U2 with a divergent filling. Thus, the variation in thickness corresponds to incising channels as well as other Oceano-sedimentological processes. As a result, we concluded that U3 was deposited in a deltaic region based on its seismic stack pattern (Dean & Dalrymple, 2001; Novico et al., 2021a, 2022b; Reineck & Singh, 1980). Unit 4 (U4), Figure 8, has a thickness of about 10 TWT (8 m) to 20 TWT (16 m) on the most recent surface that will be affected by the deposition source. Unlike other units, U4 is laterally distributed toward all study areas, but the thickness differs. The seismic facies show the rates medium to high in continuity, amplitude, and frequency, with reflector configuration mostly aggrading parallel. As an actual depositional environment, the lithofacies of U4 are generally infilled with shallow marine clay and laterally outspread by dominated clay with some intercalations of silt and fine sand from the basal layer to the top. Based on these units' interpretation, it can be determined that the geological structures are not found in this region, which means the structure of the recent fault is not identified in this region.

3.3. Sedimentologic cores and radionuclide ^{210}Pb

Drilling results BH-01 and BH-02 (Figure 6) indicate that the lithology from the seafloor to a depth of approximately 10 meters is cohesive clay sediment with a greenish-grey colour, containing remnants of clam shells, saturated with water, low plasticity, and very soft. Deeper lithology shows an alternation of sand and silt-clay deposits. Based on two boreholes, the sand pocket is 12 meters and 20 meters deep, meaning the onshore debris dominated the area in this period.

In addition to investigating coastal sediment and current condition, a radioisotope analysis of ^{210}Pb was also carried out to reveal the age of the deposition. The method

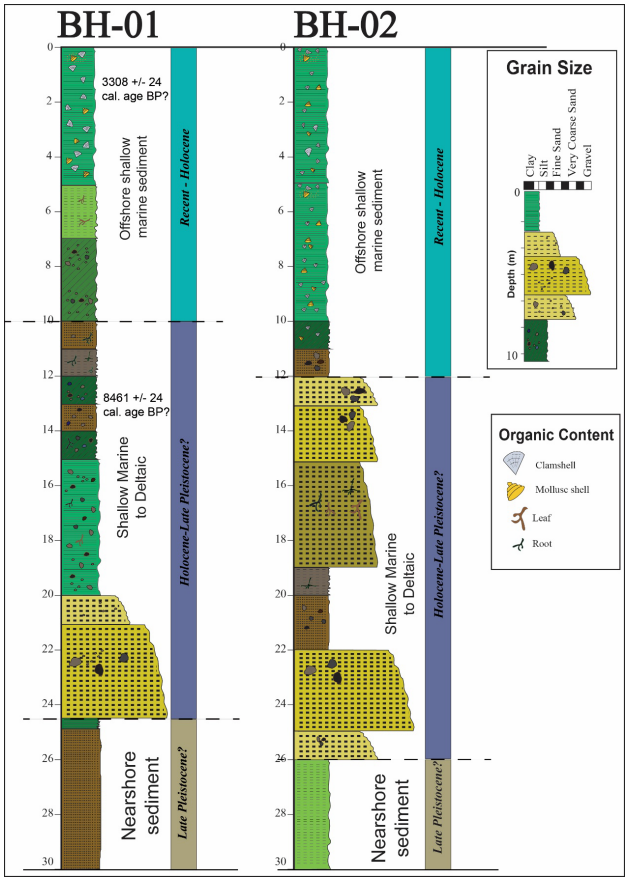

Figure 6. Core drilling BH-01 and BH-02 shows the thickness of the kind of sediment. Modified from Novico and Rahardjo (2012)

of determining the age of a deposit using a radioisotope of ^{210}Pb is widely used in global studies, particularly for deposits less than a century old (Baskaran et al., 2017; Broce et al., 2022; Páez-Osuna & Mandelli, 1985). According to the results of the sedimentation rate calculation of the selected sample, the average vertical sedimentation velocity ranges from 0.12 to 0.33 cm/year. Table 3 shows the age of deposition, which can be linked with a decade-long DSAS analysis to provide an overview of the state of the deposition trend across the Cirebon coast. Based on the velocity of sedimentation rate of CRBKJ-1 of 0.33 cm/year with deposition in 1997, it can be classified into DSAS in 1998–2008, considering that the sample was taken in 2006. Furthermore, CRBKJ-2, with a sedimentation rate of 0.32 cm/year, was connected with DSAS analysis from 1988 to 1998, whereas CRBKJ-3, with a deposition rate of 0.27 in 1977, was correlated with DSAS data from 1978 to 1988.

3.4. Hydrodynamic condition

The hydrodynamic condition simulation was conducted within one year of the monsoon condition. The hindcasting model was verified by the tidal and current parameters (Novico, 2006) to achieve a reliable model to illustrate the magnitude and direction of current speed. The Mike21 HD FM assisted with the hindcasting, and the models were completed by east-west monsoon scenarios that used recent bathymetry data from the 2018 survey, open boundaries generated by the tidal model Global Tide Model, and wind data from Jatiwangi Station from 2008 to 2018. Figure 7 shows that the current speed of the west

Table 3. The analysis of ^{210}Pb and ^{226}Ra

No	Code	Depth (cm)	Average date Estimation (year)	Estimation year of deposition	Sedimentation rate (cm/year)
1	CRBKJ-1	0–3	9.371	1997	0.33
2	CRBKJ-2	3–6	18.537	1987	0.32
3	CRBKJ-3	6–9	29.149	1977	0.27
4	CRBKJ-4	9–12	46.988	1959	0.17
5	CRBKJ-5	12–15	72.100	1934	0.12
6	CRBKJ-6	15–18	115.207	1891	0.07

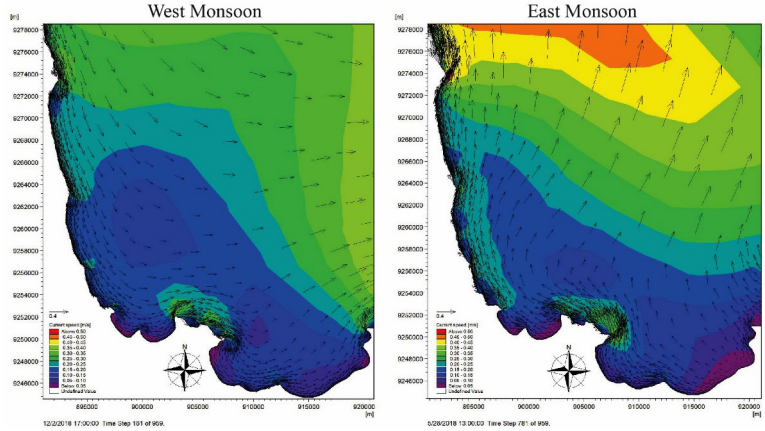

Figure 7. West and East Monsoons HD-FM 1 year Hindcasting simulation of 2018–2019

monsoon is a little smaller than the east monsoon. The top average current speed in the west monsoon is about 0.4 m/sec, and in the east monsoon, less than 0.5 m/sec, the dominant direction for both seasons is south and north, following the shoreline, which means LST. Nevertheless, the current pattern around the eastern part of the Cimanis river mouth (zone H) indicates that this area is subject to high turbulence energy of water mass.

4. Discussion

Based on the result part, the dominant pattern of the coastal landscape in Cirebon bay tends to be deposed and advanced shoreline. DSAS presents the coastline development growth almost within the entire region. The sedimentation rate supports that it has reached 0.33 cm/year since 1997, dominated by cohesive sediment, as mentioned in Figure 8. Previous researchers proved tidal and longshore currents might cause this cohesive deposition (George et al., 2019; Restrepo et al., 2016; Schaffner et al., 2001). Moreover, the hydrodynamic simulation has shown a low current magnitude for both seasons, less than 0.5 m/sec, which means cohesive sediment deposition occurred at low energy current speed. Based on the seismic record also displayed the modern deposit of offshore marine sediment identified as the thick of Recent to Holocene sediment, and the seismic record show there is no indication of uplift that is present in the seismic record.

Regionally, this phenomenon is in stark contrast to the rest of Java's northern coast, which is dominated by erosion (Ervita & Marfai, 2017; Novico et al., 2021c; Restrepo et al., 2016). This regional pattern is similar to the Cirebon coast within the 1988 to 2008 period when EPR and NSM decreased. This two-decade pattern could be aligned with the 18.6-year tidal cycle (Yasuda, 2018), which describes that the LST in this period depends on the oceanography condition. In addition, the coastline irregularity along Cirebon Bay still impacts uneven sedimentation patterns that occur along the coastline. As shown in Figure 4, Zone H experienced decade-long erosion showing sediment transport affected by shoreline differences (Van Rijn, 2011). Nevertheless, serious attention needs to be paid to the total area of the advanced coast in Cirebon Bay since the advanced coast may still occur.

Conclusions

The DSAS results show a change in the coastline from 1978 to 2018. During that period, the deposition trend dominated along the Cirebon coastline. Based on the high-resolution seismic record, it also can be seen that the deposition trend occurred in unit 4 as the top unit representing the Recent-Holocene sediment. BH-01 and BH-02 also proved that until 10m depth, it was still dominated by cohesive sediment. Verified by the ^{210}Pb radioisotope analysis, the average depositional velocity for 1978–2018

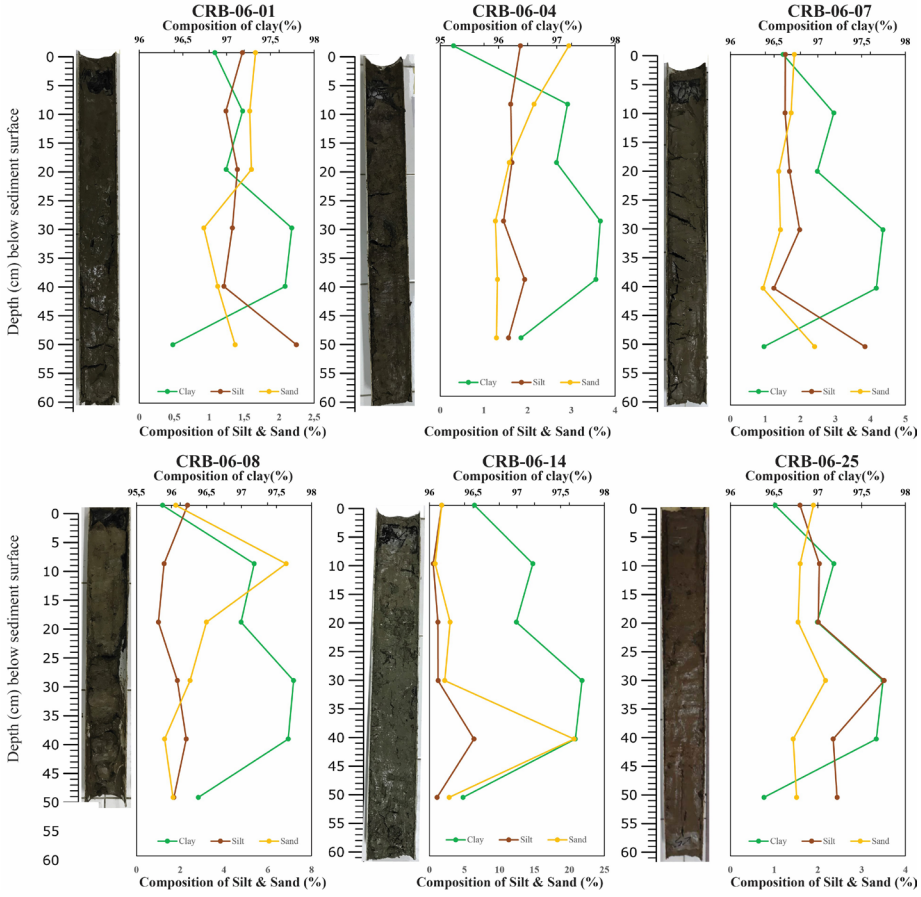

Figure 8. Sediment Grain Size distribution in the coastal zone of Cirebon

is 0.306 cm/year. Therefore, within 40 years, deposition can be seen in at least 12 cm seafloor sediment samples. For all gravity core data, the dominance of clay and silt can be recognised from the top to 20 cm sediment sample depth. Based on these conditions, the LST regime in Cirebon Bay is more affected by offshore parameters than river discharge, as evidenced by the deposition of cohesive sediment in the coastal area of Cirebon. We urge the contribution of other comprehensive topographical-tidal measurements, river discharge, and water quality information since they will be necessary for future studies on the coastal landscape.

Acknowledgements

The authors would like to thank the Marine Geological Research and Development Center-Ministry of Energy and Mineral Resources Republic of Indonesia for the support and allowance to use all data.

Funding

The field activities were fully supported by the Marine Geological Institute-Ministry of Energy and Mineral Resources Republic of Indonesia, under contract number No. 185/LAP/PPKPSL/P3GL/VI/2006.

Author contributions

Conceptualisation, RYP, FN, NS, ES, and TYMI; methodology, RYP, FN, NS, ES, and TYMI; software, RYP, and FN; validation, RYP, and FN; investigation, FN, ES, EHS, and RYP; writing original draft preparation, RYP, FN, NS, ES, TYMI, Z., EHS, and DR. All authors have read and agreed to the published version of the manuscript.

Conflicts of interest

The authors declare no conflict of interest.

References

Andreas, H., Abidin, H. Z., Sarsito, D. A., & Pradipta, D. (2018). Adaptation of 'early climate change disaster' to the northern coast of Java Island Indonesia. *Engineering Journal*, *22*(3), 207–219. https://doi.org/10.4186/ej.2018.22.3.207

Baskaran, M., Bianchi, T. S., & Filley, T. R. (2017). Inconsistencies between ^{14}C and short-lived radionuclides-based sediment accumulation rates: Effects of long-term reminer-alisation. *Journal of Environmental Radioactivity*, *174*, 10–16. https://doi.org/10.1016/j.jenvrad.2016.07.028

Boak, E. H., & Turner, I. L. (2005). Shoreline definition and detection: A review. *Journal of Coastal Research*, *214*, 688–703. https://doi.org/10.2112/03-0071.1

Broce, K., Ruiz-Fernández, A. C., Batista, A., Franco-Ábrego, A. K., Sanchez-Cabeza, J. A., Pérez-Bernal, L. H., & Guerra-Chanis, G. E. (2022). Background concentrations and accumulation rates in sediments of pristine tropical environments. *Catena*, *214*, 106252. https://doi.org/10.1016/j.catena.2022.106252

Catuneanu, O., Abreub, V., Bhattacharya, J. P., Blum, M. D., Dalrymple, R. W., Eriksson, P. G., Fielding, C. R., Fisher, W. L., Galloway, W. E., Gibling, M. R., Giles, K. A., Holbrook, J. M., Jordan, R., Kendall, C. G. S. C., Macurda, B., Martinsen, O. J., Miall, A. D., Neal, J. E., Nummedal, D., … Winker, C. (2009). Towards the standardization of sequence stratigraphy towards the standardization of sequence stratigraphy. *Earth Science Reviews*, *92*, 1–33. https://doi.org/10.1016/j.earscirev.2008.10.003

Dadson, I. Y., Owusu, A. B., & Adams, O. (2016). Analysis of shoreline change along cape coast-sekondi coast, Ghana. *Geography Journal*, *2016*, 1868936. https://doi.org/10.1155/2016/1868936

Darman, H., & Sidi, F. H. (2000). *An outline of the geology of Indonesia* (H. Darman & F. Hasan Sidi, Eds.). Indonesian Association of Geologists.

Dean, R. G., & Dalrymple, R. A. (2001). *Coastal processes with engineering applications*. Cambridge University Press. https://doi.org/10.1017/CBO9780511754500

Dolan, R., Fenster, M. S., & Holme, S. J. (1991). Temporal analysis of shoreline recession and accretion. *Journal of Coastal Research*, *7*(3), 723–744. http://www.jstor.org/stable/4297888

Ervita, K., & Marfai, M. A. (2017). Shoreline change analysis in Demak, Indonesia. *Journal of Environmental Protection*, *8*(8), 940–955. https://doi.org/10.4236/jep.2017.88059

Gardel, A., & Gratiot, N. (2006). Monitoring of coastal dynamics in French Guiana from 16 years of SPOT satellite images. *Journal of Coastal Research*, *3*(39), 1502–1505.

George, J., Sanil Kumar, V., Victor, G., & Gowthaman, R. (2019). Variability of the local wave regime and the wave-induced sediment transport along the Ganpatipule coast, eastern Arabian Sea. *Regional Studies in Marine Science*, *31*, 100759. https://doi.org/10.1016/j.rsma.2019.100759

Hamilton, W. B. (1979). *Tectonics of the Indonesian Region* (Professional Paper 1078). U.S. Govt. Print. Off. https://doi.org/10.3133/pp1078

Höffken, J., Vafeidis, A. T., MacPherson, L. R., & Dangendorf, S. (2020). Effects of the temporal variability of storm surges on coastal flooding. *Frontiers in Marine Science*, *7*, 1–14. https://doi.org/10.3389/fmars.2020.00098

Jones, G. W. (2013). *The 2010–2035 Indonesian population projection: Understanding the causes, consequences and policy options for population and development*. UNFPA Indonesia. https://indonesia.unfpa.org/en/publications?page=0%2C8

Kaczmarek, L. M., Ostrowski, R., Pruszak, Z., & Rozynski, G. (2005). Selected problems of sediment transport and morphodynamics of a multi-bar nearshore zone. *Estuarine, Coastal and Shelf Science*, *62*(3), 415–425. https://doi.org/10.1016/j.ecss.2004.09.006

Kumar, A., Narayana, A. C., & Jayappa, K. S. (2010). Shoreline changes and morphology of spits along southern Karnataka, west coast of India: A remote sensing and statistics-based approach. *Geomorphology*, *120*(3–4), 133–152. https://doi.org/10.1016/j.geomorph.2010.02.023

Kumaravel, S., Ramkumar, T., Gurunanam, B., Suresh, M., & Dharanirajan, K. (2013). An application of remote sensing and GIS based shoreline change studies – A case study in the Cuddalore district, East Coast of Tamilnadu, South India. *International Journal of Innovative Technology and Exploring Engineering (IJITEE)*, *2*(4), 211–216.

Kurt, S., Karaburun, A., & Demirci, A. (2010). Coastline changes in Istanbul between 1987 and 2007. *Scientific Research and Essays*, *5*(19), 3009–3017.

Li, W., & Gong, P. (2016). Continuous monitoring of coastline dynamics in western Florida with a 30-year time series of Landsat imagery. *Remote Sensing of Environment*, *179*, 196–209. https://doi.org/10.1016/j.rse.2016.03.031

Longuet-Higgins, M. S. (1970). Longshore currents generated by obliquely incident sea waves: 2. *Journal of Geophysical Research*, *75*(33), 6790–6801. https://doi.org/10.1029/JC075i033p06790

Martínez-Carreño, N., & García-Gil, S. (2017). Reinterpretation of the Quaternary sedimentary infill of the Ría de Vigo, NW Iberian Peninsula, as a compound incised valley. *Quaternary Science Reviews*, *173*, 124–144. https://doi.org/10.1016/j.quascirev.2017.08.015

Menier, D., Tessier, B., Proust, J. N., Baltzer, A., Sorrel, P., & Traini, C. (2010). The Holocene transgression as recorded by incised-valley infilling in a rocky coast context with low sediment supply (southern Brittany, western france). *Bulletin de La Societe Geologique de France*, *181*(2), 115–128. https://doi.org/10.2113/gssgfbull.181.2.115

Meyssignac, B., & Cazenave, A. (2012). Sea level: A review of present-day and recent-past changes and variability. *Journal of Geodynamics*, *58*, 96–109. https://doi.org/10.1016/j.jog.2012.03.005

Novico, F. (2006). *Pengembangan Pusat Penelitian dan Pengembangan Geologi Kelautan Cirebon sebagai Marine Center Tahap II*.

Novico, F., & Rahardjo, P. (2012). Desain Kapasitas Tiang Pancang Bulat Pada Lapis Sedimen Kohesif di Perairan Pantai Utara Cirebon Pada Rencana As Jetty Marine Center PPPGL Cirebon Jawa Barat. *Jurnal Geologi Kelautan*, *10*(1). https://doi.org/10.32693/jgk.10.2.2012.219

Novico, F., Endyana, C., Menier, D., Mathew, M., Kurniawan, I., Bachtiar, H., Ranawijaya, D., & Hendarmawan, H. (2021a). The dynamic coastal evidence of Jakarta Bay during Late Pleistocene-Recent. *IOP Conference Series: Earth and Environmental Science*, *930*(1), 1–13. https://doi.org/10.1088/1755-1315/930/1/012002

Novico, F., Menier, D., Mathew, M., Ramkumar, M., Santosh, M., Endyana, C., Dewi, K. T., Kurniawan, I., Lambert, C., Goubert, E., & Hendarmawan. (2021b). Impact of Late Quaternary climatic fluctuations on coastal systems: Evidence from high-resolution geophysical, sedimentological and geochronological data from the Java Island. *Marine and Petroleum Geology*, *136*, 105399. https://doi.org/10.1016/j.marpetgeo.2021.105399

Novico, F., Siddik, D. A., Lufiandi, Albab, A., Mulia, A., Kusnida, D., Komarudin, R. A., Ranawijaya, D., Kamariah, I., Endyana, C., Bachtiar, H., & Hendarmawan. (2021c). Interdisciplinary approach for qualitatively monitoring coastline dynamics in North Java Coast, Case study: Karawang Regency Indonesia. *IOP Conference Series: Earth and Environmental Science*, *944*(1), 012050. https://doi.org/10.1088/1755-1315/944/1/012050

Páez-Osuna, F., & Mandelli, E. F. (1985). ^{210}Pb in a tropical coastal lagoon sediment core. *Estuarine, Coastal and Shelf Science*, *20*(3), 367–374. https://doi.org/10.1016/0272-7714(85)90048-4

Pian, S., & Menier, D. (2011). The use of a geodatabase to carry out a multivariate analysis of coastline variations at various time and space scales. *Journal of Coastal Research*, (64), 1722–1726.

Pilkey, O. H., & Cooper, J. A. G. (2014). Are natural beaches facing extinction? *Journal of Coastal Research*, *70*, 431–436. https://doi.org/10.2112/SI70-073.1

Quang, D. N., Ngan, V. H., Tam, H. S., Viet, N. T., Tinh, N. X., & Tanaka, H. (2021). Long-term shoreline evolution using dsas technique: A case study of Quang Nam province, Vietnam. *Journal of Marine Science and Engineering*, *9*(10), 1124. https://doi.org/10.3390/jmse9101124

Reineck, H., & Singh, I. (1980). *Depositional sedimentary environments*. Springer-Verlag. https://doi.org/10.1007/978-3-642-81498-3

Restrepo, J. C., Schrottke, K., Traini, C., Ortíz, J. C., Orejarena, A., Otero, L., Higgins, A., & Marriaga, L. (2016). Sediment transport and geomorphological change in a high-discharge tropical delta (Magdalena River, Colombia): Insights from a period of intense change and human intervention (1990-2010). *Journal of Coastal Research*, *32*(3), 575–589. https://doi.org/10.2112/JCOASTRES-D-14-00263.1

Rizzo, A., & Anfuso, G. (2020). Coastal dynamic and evolution: Case studies from different sites around the world. *Water*, *12*(10), 2829. https://doi.org/10.3390/w12102829

Salahuddin, M., Astjario, P., & Lubis, S. (2001). *Compilation map of surficial sediment distribution of the Java Sea, Western Indonesian Waters*.

Sathiamurthy, E., & Voris, K. H. (2006). Maps of Holocene sea level transgression and submerged lakes on the Sunda Shelf. *The Natural History Journal of Chulalongkorn University*, *2*, 1–44.

Schaffner, L. C., Dellapenna, T. M., Hinchey, E. K., Friedrichs, C. T., Neubauer, M. T., Smith, M. E., & Kuehl, S. A. (2001). Physical energy regimes, seabed dynamics, and organism-sediment interactions along an estuarine gradient. *Organism-Sediment Interactions*, *21*, 159–179.

Silitonga, P. H., & Masria, M. (1978). *Geological map of the Cirebon quadrangle, West Java 1:100.000*. GRDC, Bandung.

Thieler, E. R., Himmelstoss, E. A., Zichichi, J. L., & Ergul, A. (2009). *The Digital Shoreline Analysis System (DSAS) Version 4.0 – An ArcGIS extension for calculating shoreline change*. U.S. Geological Survey. https://doi.org/10.3133/ofr20081278

Toorman, E. A., Anthony, E., Augustinus, P. G. E. F., Gardel, A., Gratiot, N., Homenauth, O., Huybrechts, N., Monbaliu, J., Moseley, K., & Naipal, S. (2018). Interaction of mangroves, coastal hydrodynamics, and morphodynamics along the coastal fringes of the Guianas. In *Coastal Research Library* (Vol. 25). Springer. https://doi.org/10.1007/978-3-319-73016-5_20

Vail, P. R., Mitchum, R. M., & Thompson, S. (1977). Seismic stratigraphy and global change in sea level, part 3: Relative change of sea level from coastal onlap. In C. E. Payton (Ed.), *Seismic stratigraphy – Applications to hydrocarbon exploration, American Association of Petroleum Geologists: Vol. Memoir 26* (pp. 63–81).

Van Rijn, L. C. (2011). Coastal erosion and control. *Ocean and Coastal Management*, *54*(12), 867–887. https://doi.org/10.1016/j.ocecoaman.2011.05.004

van Rijn, L. C., Wasltra, D. J. R., Grasmeijer, B., Sutherland, J., Pan, S., & Sierra, J. P. (2003). The predictability of cross-shore bed evolution of sandy beaches at the time scale of storms and seasons using process-based profile models. *Coastal Engineering*, *47*(3), 295–327. https://doi.org/10.1016/S0378-3839(02)00120-5

Vos, K., Harley, M. D., Splinter, K. D., Simmons, J. A., & Turner, I. L. (2019). Sub-annual to multi-decadal shoreline variability from publicly available satellite imagery. *Coastal Engineering*, *150*, 160–174. https://doi.org/10.1016/j.coastaleng.2019.04.004

Williams, S. J. (2013). Sea-level rise implications for coastal regions. *Journal of Coastal Research*, *63*, 184–196. https://doi.org/10.2112/SI63-015.1

Xu, N. (2018). Detecting coastline change with all available landsat data over 1986-2015: A case study for the state of Texas, USA. *Atmosphere*, *9*(3), 107. https://doi.org/10.3390/atmos9030107

Yasuda, I. (2018). Impact of the astronomical lunar 18.6-yr tidal cycle on El-Niño and Southern Oscillation. *Scientific Reports*, *8*(1), 4–11. https://doi.org/10.1038/s41598-018-33526-4